


ARTICLE

Open Access

MiR-215-5p is a tumor suppressor in colorectal cancer targeting EGFR ligand epiregulin and its transcriptional inducer HOXB9

Petra Vychytilova-Faltejskova^{1,2}, Jana Merhautova^{1,3}, Tana Machackova¹, Irene Gutierrez-Garcia⁴, José Garcia-Solano⁵, Lenka Radova¹, Dominika Brchnelova¹, Katerina Slaba¹, Marek Svoboda^{1,2}, Jana Halamkova², Regina Demlova³, Igor Kiss², Rostislav Vyzula², Pablo Conesa-Zamora⁴ and Ondrej Slaby^{1,2} 

Abstract

Growing evidence suggests that microRNAs are involved in the development and progression of colorectal cancer (CRC). In the present study, deregulation and functioning of tumor-suppressive miR-215-5p was evaluated in CRC. In total, 448 tumor tissues and 325 paired adjacent healthy tissues collected from Czech and Spain cohorts of CRC patients have been used for miR-215-5p expression analyses. A series of in vitro experiments have been performed using transient transfection of miR-215-5p mimics into four CRC cell lines to identify specific cellular processes affected by miR-215-5p. Further, the effects of miR-215-5p on tumor growth were evaluated in vivo using NSG mice and stable cell line overexpressing miR-215-5p. Target mRNAs of miR-215-5p were tested using luciferase assay and western blot analyses. We found that miR-215-5p is significantly downregulated in tumor tissues compared with non-tumor adjacent tissues and its decreased levels correlate with the presence of lymph node metastases, tumor stage, and shorter overall survival in CRC patients. Overexpression of miR-215-5p significantly reduced proliferation, clonogenicity, and migration of CRC cells, lead to cell cycle arrest in G2/M phase and p53-dependent induction of apoptosis. The ability of miR-215-5p to inhibit tumor growth was confirmed in vivo. Finally, we confirmed epiregulin and HOXB9 to be the direct targets of miR-215-5p. As epiregulin is EGFR ligand and HOXB9 is its transcriptional inducer, we suggest that the main molecular link between miR-215-5p and CRC cells phenotypes presents the EGFR signaling pathway, which is one of the canonical pathogenic pathways in CRC.

Introduction

Colorectal cancer (CRC) is the third most common cancer worldwide and the fourth leading cause of cancer related deaths. Despite the fact that the incidence and mortality rates have been steadily declining, >50% of all patients with CRC will die of the disease¹. In recent years,

many different classes of non-coding RNAs have been identified as key regulators of various cellular processes including cell proliferation, differentiation, apoptosis or migration^{2–5}. MicroRNAs (miRNAs) are short single-stranded non-coding RNAs that post-transcriptionally regulate gene expression by binding to 3' untranslated regions of target mRNAs⁶. Many studies have shown they can act as both oncogenes and tumor suppressors and their deregulation has been associated with the initiation and progression of a wide range of human diseases, including cancer^{7, 8}. In addition, association between

Correspondence: Ondrej Slaby (on.slaby@gmail.com)

¹Central European Institute of Technology, Masaryk University, Brno, Czech Republic

²Department of Comprehensive Cancer Care, Masaryk Memorial Cancer Institute, Faculty of Medicine, Masaryk University, Brno, Czech Republic
Full list of author information is available at the end of the article

© The Author(s). 2017



Open Access This article is licensed under a Creative Commons Attribution 4.0 International License, which permits use, sharing, adaptation, distribution and reproduction in any medium or format, as long as you give appropriate credit to the original author(s) and the source, provide a link to the Creative Commons license, and indicate if changes were made. The images or other third party material in this article are included in the article's Creative Commons license, unless indicated otherwise in a credit line to the material. If material is not included in the article's Creative Commons license and your intended use is not permitted by statutory regulation or exceeds the permitted use, you will need to obtain permission directly from the copyright holder. To view a copy of this license, visit <http://creativecommons.org/licenses/by/4.0/>.

miRNA expression, prognosis and therapy response prediction was repeatedly described^{9, 10}.

Over the past decade, several miRNAs with deregulated expression in CRC have been identified, including miR-215-5p^{11–15}. We focus on miR-215-5p as we identified this miRNA to be downregulated in colorectal tumor tissue in our previous work¹¹, where it indicated also promising tumor-suppressive features in preliminary *in vitro* functional screen¹¹. In general, this miRNA is supposed to function as a tumor suppressor and its levels are often downregulated in tumor tissues. However, its role in CRC pathogenesis has not been fully elucidated yet. In 2008, miR-215 has been shown to act as an effector as well as regulator of p53¹³. Further, denticleless protein homolog¹⁴ and thymidylate synthase¹⁵ were confirmed to be the miR-215-5p targets. Low expression levels of miR-215-5p were associated with resistance to 5-fluorouracil-containing adjuvant chemotherapy¹⁶. Finally, the deregulation of this miRNA is supposed to be a very early event, which is not dependent on the mechanism of initiation of transformation, suggesting that miR-215-5p is likely to regulate critical signaling pathways that are crucial for early transformation of colonic epithelial cells¹².

In this study, we have determined expression levels of miR-215-5p in two large independent cohorts of CRC patients to confirm its downregulation in tumor tissue and prognostic potential. To further discover the role of miR-215-5p in CRC pathogenesis, we have performed deep *in vitro* analyses with the aim to describe the most significantly affected CRC cells phenotypes and identify mRNA targets and the key signaling pathways affected by miR-215-5p. The role of miR-215-5p in regulation of tumor growth was evaluated also *in vivo* using mouse model.

Results

miR-215-5p is downregulated in CRC tissues and its low levels correlate with aggressive disease

It was confirmed that the expression of miR-215-5p is significantly downregulated in tumor tissue compared with adjacent mucosa ($P < 0.0001$; Fig. 1a) in case of Czech cohort (Table 1). In addition, the levels of miR-215-5p decreased progressively with advanced clinical stages ($P < 0.0001$; Fig. 1c) and low expression was associated with lymph nodes positivity ($P < 0.0001$; Supplementary Fig. S1A). Further, significantly downregulated levels of miR-215-5p were found not only in primary tumors, but also in corresponding liver metastases ($P < 0.0001$; Supplementary Fig. S1B). Survival analyses proved that patients with low levels of miR-215-5p have significantly shorter overall survival (OS) ($P = 0.0024$; cut-off 0.02393; Fig. 1e) compared with patients with higher expression levels.

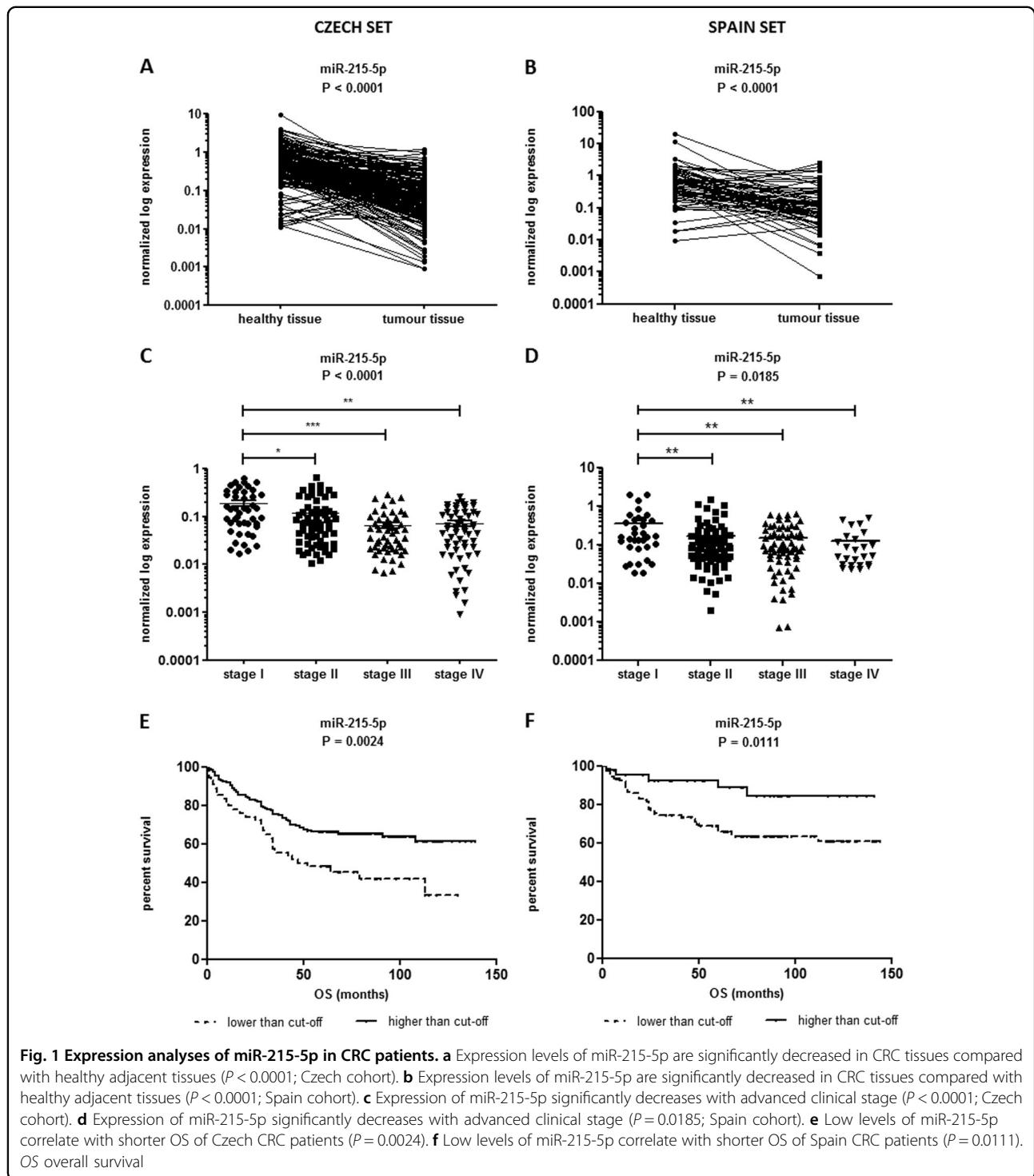
To further validate these observations, an independent cohort from Spain was included in the study (Table 1). As in the Czech cohort, the expression of miR-215-5p was significantly downregulated in tumor tissues ($P < 0.0001$; Fig. 1b) and its low levels were associated with advanced clinical stage ($P = 0.0185$; Fig. 1d), but not with the lymph node positivity (Table 1). Again, the low levels of miR-215-5p were associated with shorter OS and worse prognosis of CRC patients ($P = 0.0111$; cut-off 0.2139; Fig. 1f).

miR-215-5p expression levels in CRC cells

miR-215-5p expression levels in CRC cells used in our study was performed by use of calibration curve (Supplementary Fig. S7A) and absolute quantification. The number of miR-215-5p copies varied among CRC cells (Supplementary Fig. S7B). HCT-116^{+/+}, HCT-116^{-/-}, DLD-1 and HT-29 were characteristic with very low number of miR-215-5p copies ranging from 1351 to 3639 copies per 100 ng of total RNA purified from CRC cells. On the contrary, the only CRC cells indicating multiple time higher levels were CaCo2 cells with number of copies 98 962 per 100 ng of total RNA. Based on this results, HCT-116^{+/+}, HCT-116^{-/-}, DLD-1 and HT-29 cells were used as models for miR-215-5p substitution and CaCo2 for miR-215-5p silencing.

miR-215-5p inhibits proliferation, viability and colony formation of CRC cells

By transfection of miR-215-5p, mimic reached significant increase of miR-215-5p levels in all studied cell lines, which was stable from 24 to 96 h. Expression levels of miR-215-5p in cells transfected with miR-215-5p mimic were 8000–10 000 times higher when compared with mock-transfected control cells. Cell counting demonstrated cell proliferation to be inhibited by ectopic expression of miR-215-5p, with the best inhibition effect being observed 96 h after transfection ($P < 0.001$ for HCT-116^{+/+} and HT-29; $P < 0.01$ for DLD-1 and HCT-116^{-/-}; Figs. 2a, b, Supplementary Figs. S2A, B). Parallel to cell counting, MTT (3-(4,5-dimethylthiazol-2-yl)-2,5-diphenyltetrazolium bromid) assay was performed to assess the effect of miR-215-5p on cell viability. Similarly to the previous results, the viability of CRC cells was significantly reduced 96 h after transfection ($P < 0.001$ for HCT-116^{+/+} and HT-29; $P < 0.01$ for DLD-1; $P < 0.05$ for HCT-116^{-/-}). To determine whether the alterations in cell proliferation and viability were the result of cell cycle regulation, flow cytometry was used. Ninety-six hours after transfection, miR-215-5p decreased the proportion of HCT-116^{+/+} (Fig. 2c), HCT-116^{-/-} (Supplementary Fig. S2C) and DLD-1 (Fig. 2d) cells in the G0/G1-phase and increased the proportion of the cells in S-phase and G2/M-phase compared with those transfected with



control oligonucleotides. In case of HT-29 cells, only the arrest in G2/M-phase was observed (Supplementary Fig. S2D). To find out whether the inhibition of growth induced by miR-215-5p was anchorage independent, the cells were seeded on soft agar 24 h post-transfection. After

14 days, HCT-116^{+/+} and DLD-1 cells transfected with miR-215-5p mimics formed significantly fewer colonies than cells transfected with control oligonucleotide ($P < 0.001$; Figs. 2e, f).

Table 1 Correlation of miR-215-5p expression with clinical-pathological features of CRC patients

	<i>n</i> (%)	miR-215-5p Czech cohort median (25–75%)	<i>n</i> (%)	miR-215-5p Spain cohort median (25–75%)
Age				
Median (range)	66 (18–92)	NA	73 (36–91)	NA
Sex				
Male	139 (55)	0.07 (0.02–0.15)	107 (55)	0.07 (0.03–0.17)
Female	113 (45)	0.07 (0.03–0.014)	89 (45)	0.10 (0.04–0.20)
<i>P</i> -value		0.9673		0.3508
Tumor vs. mucosa				
Normal mucosa	252	0.51 (0.33–0.87)	73	0.58 (0.27–1.19)
Colorectal tumor	252	0.07 (0.03–0.14)	196	0.11 (0.05–0.25)
<i>P</i> -value		<0.0001		<0.0001
Clinical stage	<i>n</i> = 252		<i>n</i> = 192	
I	43 (17)	0.14 (0.07–0.31)	23 (12)	0.15 (0.09–0.43)
II	78 (31)	0.07 (0.03–0.13)	82 (43)	0.08 (0.05–0.16)
III	60 (24)	0.04 (0.02–0.08)	64 (33)	0.08 (0.04–0.20)
IV	71 (28)	0.05 (0.02–0.12)	23 (12)	0.05 (0.03–0.15)
<i>P</i> -value		<0.0001		0.0185
pT category	<i>n</i> = 252		<i>n</i> = 193	
pT1	4 (2)	0.30 (0.08–0.60)	10 (5)	0.04 (0.03–0.08)
pT2	51 (20)	0.09 (0.05–0.26)	18 (9)	0.05 (0.01–0.20)
pT3	172 (68)	0.06 (0.02–0.13)	124 (65)	0.09 (0.04–0.16)
pT4	25 (10)	0.04 (0.02–0.09)	41 (21)	0.10 (0.05–0.20)
<i>P</i> -value		0.0018		0.2515
Lymph nodes	<i>n</i> = 252		<i>n</i> = 192	
Negative	135 (54)	0.09 (0.04–0.21)	110 (57)	0.09 (0.05–0.19)
Positive	117 (46)	0.04 (0.02–0.10)	82 (43)	0.08 (0.04–0.20)
<i>P</i> -value		<0.0001		0.4397
Distant metastases	<i>n</i> = 252		<i>n</i> = 193	
No	181 (72)	0.07 (0.03–0.14)	170 (88)	0.08 (0.04–0.15)
Yes	71 (28)	0.06 (0.02–0.15)	23 (12)	0.14 (0.03–0.30)
<i>P</i> -value		0.2780		0.3306
Grading	<i>n</i> = 252		<i>n</i> = 196	
G1	67 (27)	0.07 (0.03–0.26)	144 (73)	0.09 (0.04–0.20)
G2	132 (52)	0.07 (0.03–0.12)	47 (24)	0.08 (0.04–0.14)
G3	53 (21)	0.04 (0.02–0.16)	5 (3)	0.13 (0.02–0.31)
<i>P</i> -value		0.1771		0.4259
Tumor location	<i>n</i> = 252		<i>n</i> = 194	
Proximal colon	100 (40)	0.07 (0.03–0.18)	104 (54)	0.09 (0.04–0.19)
Distal colon	152 (60)	0.07 (0.02–0.13)	90 (46)	0.07 (0.03–0.17)
<i>P</i> -value		0.4787		0.1817

The *P*-values in bold are statistically significant
 NA not applicable

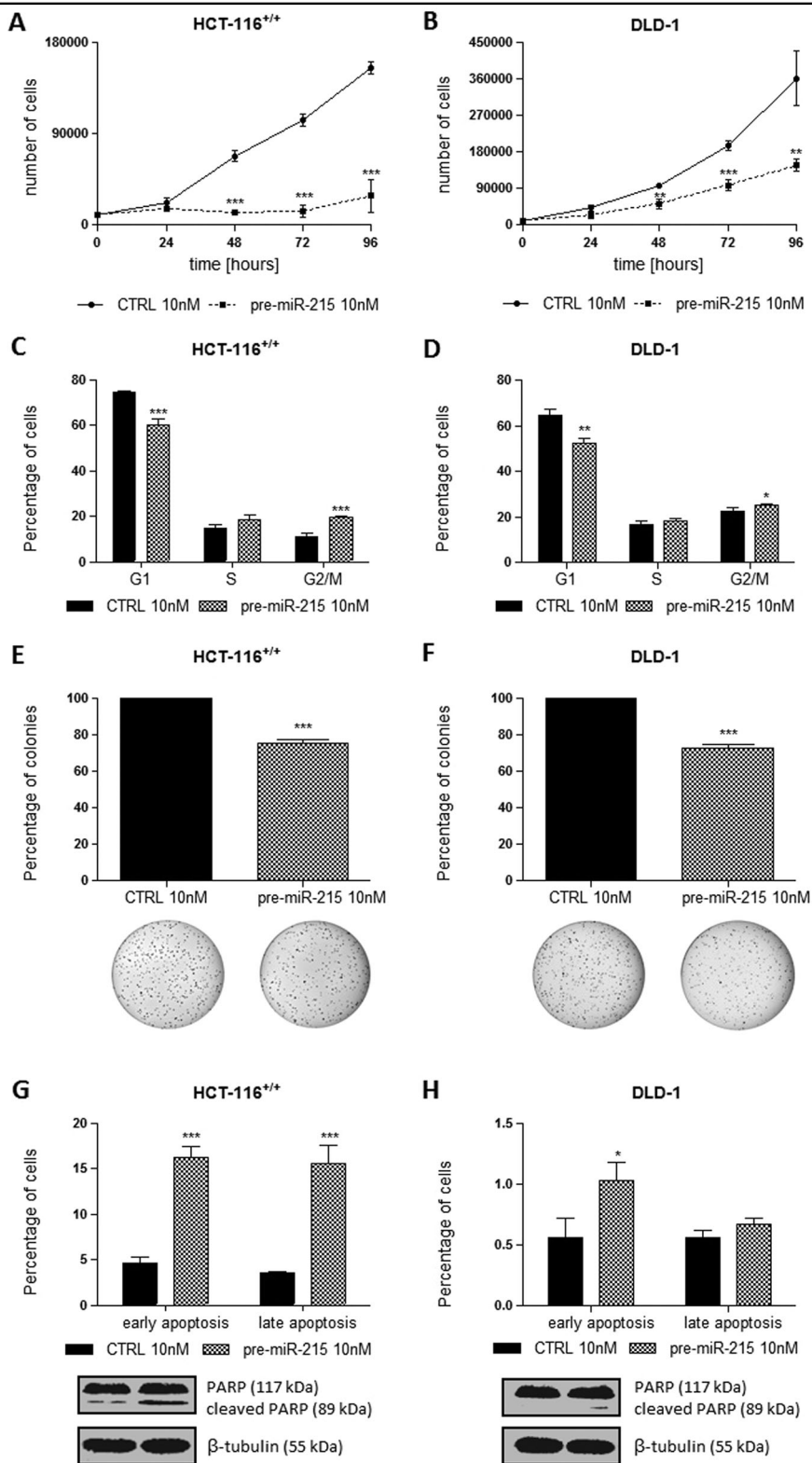


Fig. 2 (See legend on next page.)

MiR-215-5p induces apoptosis of CRC cells in a wild-type p53-dependent manner

Transfection of miR-215-5p into HCT-116^{+/+} cells (wt-p53) significantly increased the number of apoptotic cells by at least threefold ($P < 0.001$; Fig. 2g). Further, the levels of cleaved PARP were increased subsequent to transfection with miR-215-5p (Fig. 2g). Importantly, transfection of miR-215-5p mimics into HCT-116^{-/-} (p53-null), DLD-1 (mut-p53) and HT-29 (mut-p53) cells did not lead to increased apoptosis rates and elevated levels of cleaved PARP (Fig. 2h, Supplementary Figs. S2E–F).

MiR-215-5p inhibits migration of CRC cells

According to the results of scratch wound assay, transfection of miR-215-5p mimics led to a significant inhibition of cell migration ($P < 0.001$ for DLD-1, HCT-116^{+/+} and HCT-116^{-/-}; $P < 0.05$ for HT-29; Figs. 3a, b and Supplementary Figs. S3A, B). In addition, transwell migration assay confirmed significantly reduced migration of cells overexpressing miR-215-5p. The inhibition rate was $57 \pm 16\%$, $37 \pm 8\%$, and $50 \pm 17\%$, respectively, in HCT-116^{+/+} (Fig. 3c), DLD-1 (Fig. 3d), and HCT-116^{-/-} cells transfected with miR-215-5p mimics compared with control group.

REG and HOXB9 are direct targets of miR-215-5p

To better understand the role of miR-215-5p in CRC pathogenesis, the TargetScan¹⁷, DIANA-microT¹⁸, RNAhybrid¹⁹, miRanda²⁰ and RNA22²¹ databases were searched for the predicted targets of miR-215-5p associated with cell proliferation and migration. Among the target genes that were considered to be the most likely involved in these processes, epiregulin (REG)²² and HOXB9²³ have been chosen for further analyses. It was found that miR-215-5p transfection leads to the significant decrease in mRNA levels of both genes of interest (Figs. 4a–d). Subsequently, the luciferase reporter assay was utilized to confirm direct interaction between miR-215-5p and 3'-UTR of REG and HOXB9. It was shown that miR-215-5p suppressed $62 \pm 6\%$ of reporter activity of the pEZX-MT05-REG reporter compared with the control oligonucleotide, whereas the pEZX-MT05-ctrl vector was resistant to the inhibition ($P < 0.001$; Fig. 4e). Similarly, the reporter activity of the pLSG-RenSP-HOXB9 reporter was suppressed by $48 \pm 3\%$ after

transfection of miR-215-5p compared with control cells, whereas the pLSG-RenSP-ctrl vector was resistant to the inhibition ($P < 0.001$; Fig. 4f). In addition, western blot analyses proved that overexpression of miR-215-5p suppresses the expression of both proteins 48 h after transfection (Fig. 4g). To further support these data, depletion of REG and HOXB9 using small interfering RNA (siRNA)-mediated knockdown was performed (Supplementary Figs. S4A–D). It was shown that downregulation of these two proteins leads to the significant decrease in proliferation of HCT-116^{+/+} ($P < 0.001$ in case of REG, $P < 0.01$ in case of HOXB9; Supplementary Fig. S5A), HCT-116^{-/-} ($P < 0.01$ in case of REG; Supplementary Fig. S5B) and DLD-1 ($P < 0.01$ in case of REG, $P < 0.05$ in case of HOXB9; Supplementary Fig. S5C) cells 96 h after transfection. By use of scratch wound assay, we were not able to prove any significant effects of REG and HOXB9 silencing on migratory capacity of studied cells ($P > 0.05$). Finally, the levels of REG and HOXB9 were examined in the matched tumor and non-tumor tissues of CRC patients. It was shown that the expression of REG and HOXB9 is significantly increased in tumor tissues compared with healthy tissues ($P < 0.01$ for REG, $P < 0.001$ for HOXB9; Fig. 4h).

MiR-215 induces increase in E-cadherin expression

When we compared the expression levels of EMT markers (E-cadherin, vimentin, ZEB1, ZEB2) in HCT-116^{+/+}-miR-215-5p cells and HCT-116^{+/+}-control cells, we observed significantly higher levels of E-cadherin ($P = 0.0164$, Supplementary Fig. S6) in miR-215-5p-positive cells. There was no difference in vimentin and ZEB1 expression levels between studied cell lines. ZEB2 was not detectable in both cell lines.

MiR-215-5p silencing facilitate proliferation of CRC cells and induce expression of REG and HOXB9

We successfully silenced miR-215-5p expression in CaCo2 cells to 16% of its expression levels in control CaCo2 cells transfected with anti-miRNA control oligonucleotide (Supplementary Fig. S8A). Silencing of miR-215-5p by use of anti-miR-215 in CaCo2 cells led to the increase in expression levels of miR-215-5p targets REG and HOXB9 after 48 h (Supplementary Fig. S8B). Finally, decreased levels of miR-215-5p facilitated proliferation of

(see figure on previous page)

Fig. 2 Effects of miR-215-5p overexpression on HCT-116^{+/+} and DLD-1 cells. **a** miR-215-5p significantly inhibits the proliferation of HCT-116^{+/+} cells. **b** miR-215-5p significantly inhibits the proliferation of DLD-1 cells. **c** miR-215-5p significantly reduce the clonogenicity of HCT-116^{+/+} cells. **d** miR-215-5p significantly reduce the clonogenicity of DLD-1 cells. **e** Overexpression of miR-215-5p in HCT-116^{+/+} cells leads to a cell cycle arrest in G2/M phase. **f** Overexpression of miR-215-5p in DLD-1 cells leads to a cell cycle arrest in G2/M phase. **g** miR-215-5p increases the apoptosis of HCT-116^{+/+} cells in p53-dependent manner. **h** miR-215-5p increases the early apoptosis of DLD-1 cells. * $P < 0.05$, ** $P < 0.01$, *** $P < 0.001$, CTRL control cells

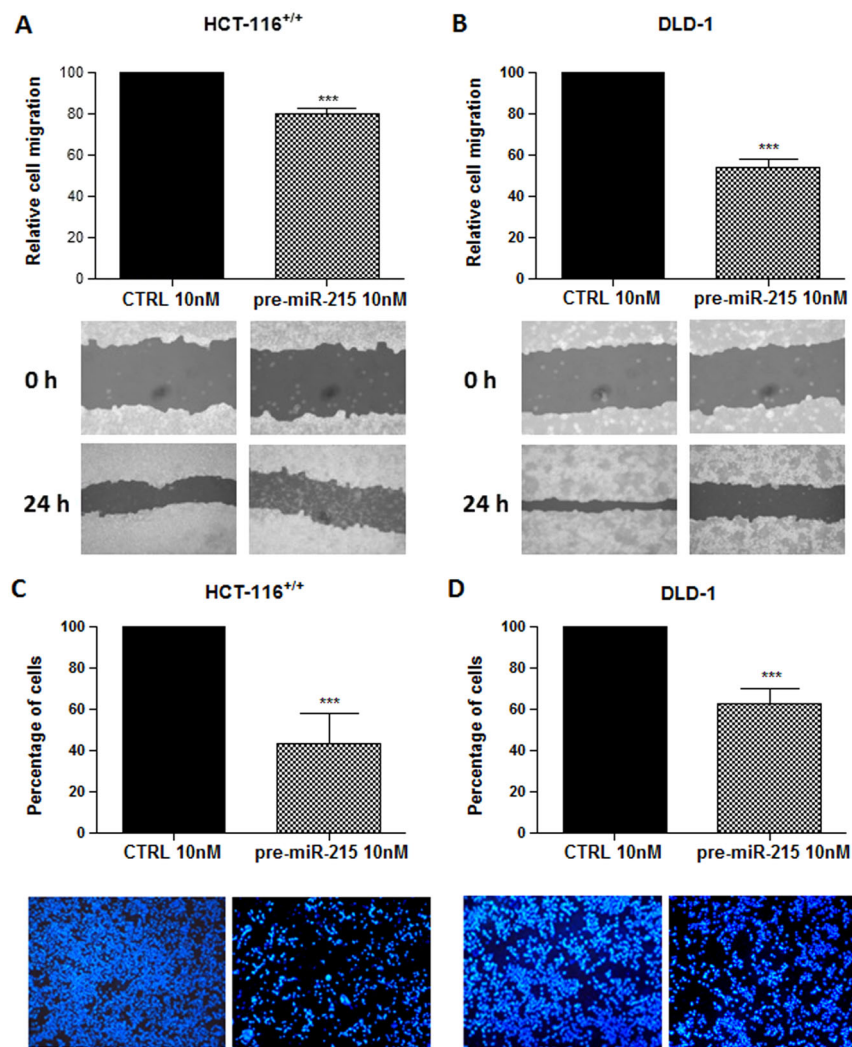


Fig. 3 Effects of miR-215-5p overexpression on migration of HCT-116^{+/+} and DLD-1 cells. **a** miR-215-5p significantly reduce the migration of HCT-116^{+/+} cells (transwell migration assay). **b** miR-215-5p significantly reduce the migration of DLD-1 cells (transwell migration assay). **c** miR-215-5p significantly reduce the migration of HCT-116^{+/+} cells (scratch wound assay). **d** miR-215-5p significantly reduce the migration of DLD-1 cells (scratch wound assay). ** $P < 0.01$, *** $P < 0.001$, CTRL control cells

CaCo2 cells, which was significant at first ($P = 0.03$) and second day ($P = 0.02$) post-transfection (Supplementary Fig. S8C). We have not observed any significant effects of miR-215-5p silencing on migratory capacity of CaCo2 cells by use scratch wound-healing assay ($P > 0.05$).

MiR-215-5p overexpression suppresses tumor growth *in vivo*

To evaluate how miR-215-5p overexpression affects tumor growth *in vivo*, subcutaneous tumors were generated in NSG mice using HCT-116^{+/+}-miR-215-5p cells and HCT-116^{+/+}-control cells. It was confirmed that HCT-116^{+/+}-control tumors grow significantly faster than the HCT-116^{+/+}-miR-215-5p tumors (Figs. 5a–c).

Importantly, reverse transcriptase-quantitative PCR (RT-qPCR) analysis showed that the expression of miR-215-5p is still upregulated in HCT-116^{+/+}-miR-215-5p tumors compared with control tumors (Fig. 5d) 25 days from the beginning of the experiment.

Discussion

Growing evidence suggests that miRNAs are involved in the development and progression of different types of human cancers^{24–26}. In 2008, miR-215-5p was first described as a tumor suppressor in CRC¹³. Since then, several other authors studied prognostic and predictive value of miR-215-5p^{14–16}; however, its detail functioning in the pathogenesis of the disease has not been clarified

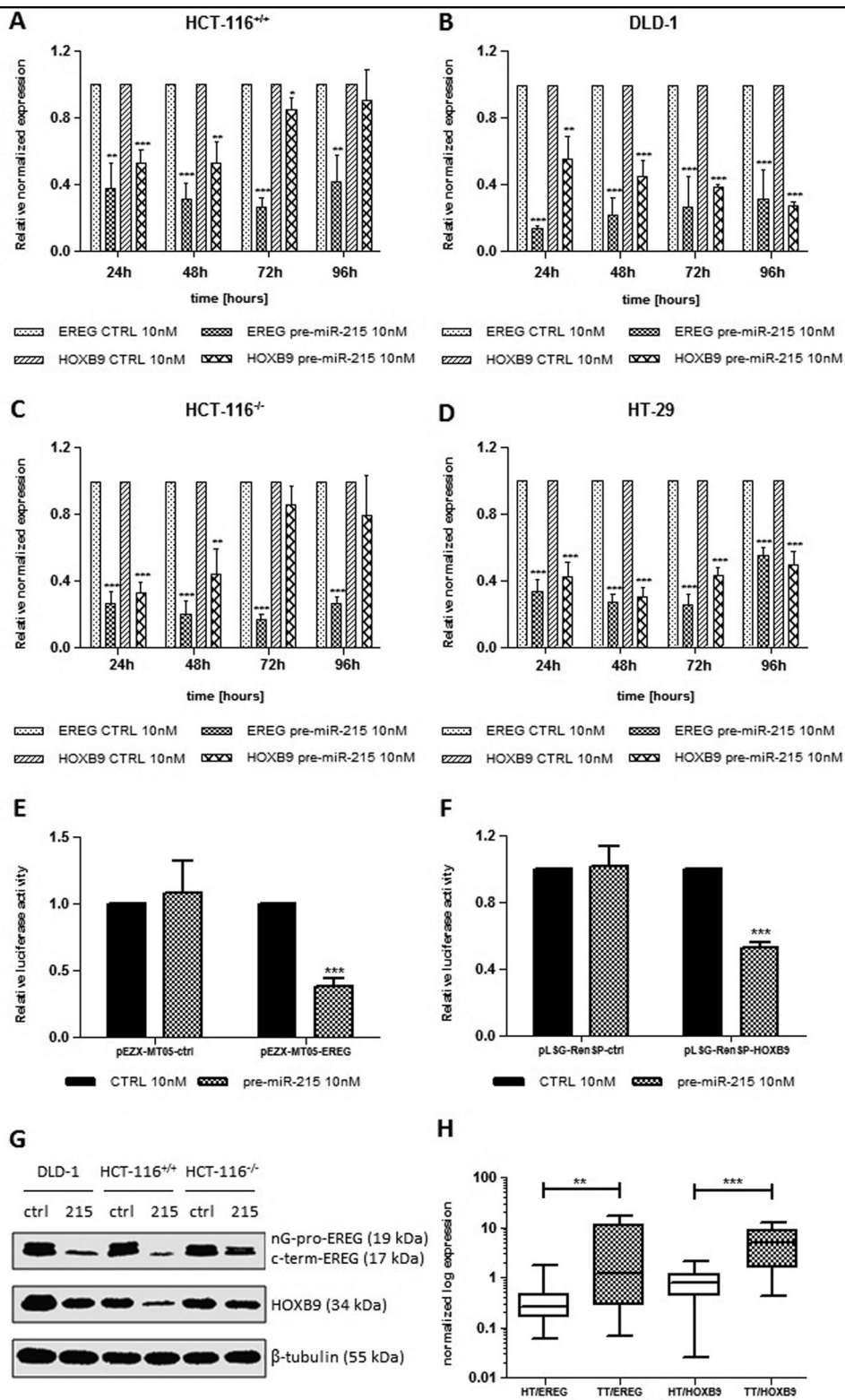


Fig. 4 (See legend on next page.)

yet. Thus, we have analyzed not only the diagnostic and prognostic potential of miR-215-5p, but we also aimed to identify its target genes and describe its involvement in CRC cells phenotypes and particular signaling pathways.

We have confirmed that the expression of miR-215-5p is significantly downregulated in tumor tissues compared with paired healthy tissues and its reduced levels correlate with higher clinical stage, presence of lymph node metastases and shorter OS. These results are in agreement with former studies^{27–30}.

To identify specific cellular processes influenced by miR-215-5p, series of in vitro experiments have been performed. The results proved that higher levels of miR-215-5p significantly reduce metabolic activity and proliferation of CRC cell lines. The opposite effects were observed when miR-215-5p silencing approach was used in CaCo2 cells, where decreased levels of miR-215-5p led to enhanced cellular proliferation. Similarly, the in vivo experiments confirmed significantly slower growth of tumors stably expressing this miRNA. In compliance with previous studies^{13, 14}, the inhibitory effect was more profound in cells containing wild-type p53 (HCT-116^{+/+}) compared with p53-mutant (DLD-1, HT-29) or p53-null (HCT-116^{-/-}) cells. On the other hand, miR-215-5p significantly reduced cell proliferation even in the absence of p53; thus it seems that this miRNA slows down the proliferation not only through the cell cycle arrest, but also by affecting another signaling pathways independent of p53 function. Concerning the cell cycle, transfection of miR-215-5p lead to the significant arrest in G2/M phase. These results again support the hypothesis of other proteins than p53 being involved in reduced proliferation. Georges et al. confirmed denticleless protein homolog to be a direct target of miR-215-5p that interacts with DDB1-CUL4 and MDM2-p53 ligase complexes and influences the stability of p53 and its target p21^{31, 32}. Similarly, Boni et al. identified thymidylate synthase as another target of miR-215-5p that was suggested to be a predictive biomarker for 5-FU response in CRC. To find out whether the inhibition of growth induced by miR-215-5p was anchorage independent, the clonogenic assay was performed¹⁵. It was revealed that number of colonies is significantly lower in case of HCT-116^{+/+} and DLD-1 cells transfected with miR-215-5p mimics, but not in

HCT-116^{-/-} and HT-29 cells indicating that this miRNA could affect the cell clone formation by mechanisms that are at least in part dependent on p53 functionality. Interestingly, although carrying out the above experiments significant morphologic changes in HCT-116^{+/+} cells transfected with miR-215-5p, such as round shape and plate surface detachment, have been repeatedly observed. These changes may have many reasons including reduced expression of adhesion molecules, loss of cell polarity, dysfunctional cytoskeleton or cell apoptosis³³. Georges et al. identified discs large homolog 5 as an important target of miR-215-5p³¹. It was shown that this protein can interfere with cell adhesion through the reduction of cadherin transport to the cell surface and it is proposed to function in the maintenance of epithelial cell structure³⁴. Concerning the effect of miR-215-5p on cell apoptosis, it was assessed that overexpression of this miRNA leads to the significant increase of apoptotic rate in case of HCT-116^{+/+} cells. Although the exact mechanism of action is not known, it was proved that this outcome is strongly dependent on the presence of wt-p53 and could be related to morphologic changes described earlier. To date, no target genes of miR-215-5p associated with cell apoptosis have been identified in CRC. Nevertheless, X-chromosome-linked inhibitor of apoptosis (XIAP) was found to be regulated by this miRNA in ovarian³⁵ and non-small cell lung cancer³⁶.

Further, we observed that higher levels of miR-215-5p lead to a significant inhibition of cell migration. Interestingly, the highest effect was determined in case of DLD-1 cell line indicating the independence of p53 status. In 2011, White et al. identified ZEB2 as a direct target of miR-215-5p in renal cell carcinoma³⁷. These results were further confirmed using non-small cell lung cancer³⁸ and pancreatic cancer³⁹ cell lines. Using the metastatic gene profiling assay, several other genes involved in the degradation of extracellular matrix or cell adhesion, such as MMP7/13 or CDH1/6/11, have been described to be affected by increased miR-215-5p expression in renal cell carcinoma³⁷; however, these targets need to be further validated in CRC.

As our observations proved significant effects of miR-215-5p on cell proliferation and migration, several databases have been searched for the potential targets of miR-

(see figure on previous page)

Fig. 4 EREG and HOXB9 are direct targets of miR-215-5p. **a** RT-qPCR analyses proved significantly reduced mRNA levels of EREG and HOXB9 in HCT-116^{+/+} cells. **b** RT-qPCR analyses proved significantly reduced mRNA levels of EREG and HOXB9 in DLD-1 cells. **c** RT-qPCR analyses proved significantly reduced mRNA levels of EREG and HOXB9 in HCT-116^{-/-} cells. **d** RT-qPCR analyses proved significantly reduced mRNA levels of EREG and HOXB9 in HT-29 cells. **e** Luciferase assay confirmed EREG to be a direct target of miR-215-5p. **f** Luciferase assay confirmed HOXB9 to be a direct target of miR-215-5p. **g** Western blot analyses proved downregulated protein levels of EREG and HOXB9 in CRC cells transfected with miR-215-5p mimics. **h** Expression of EREG and HOXB9 is significantly upregulated in tumor tissues compared with non-tumor adjacent tissues. **P* < 0.05, ***P* < 0.01, ****P* < 0.001, CTRL control cells, HT healthy tissue, TT tumor tissue

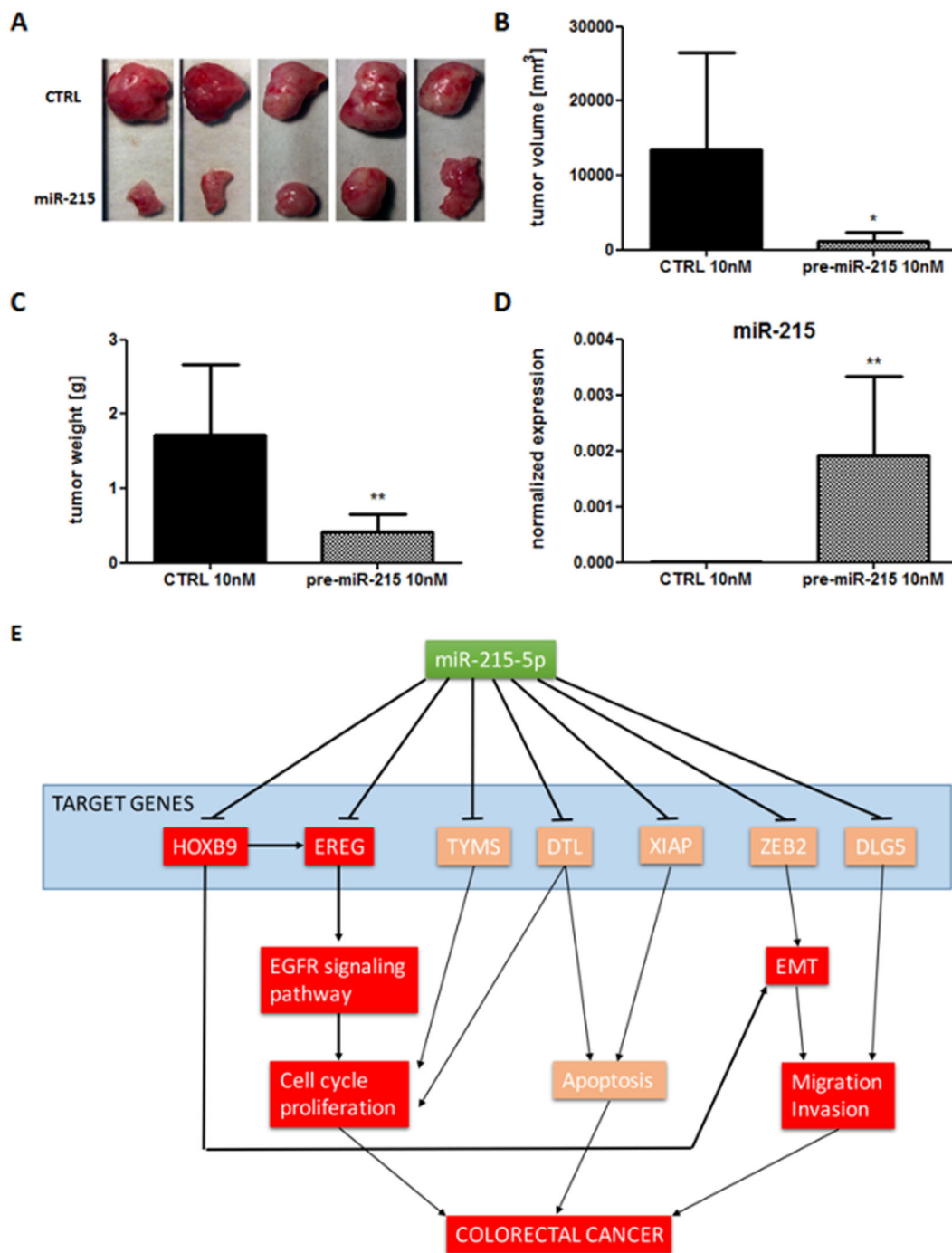


Fig. 5 Effects of miR-215-5p overexpression on tumor growth *in vivo* and its involvement in CRC pathogenesis. **a** Subcutaneously injected HCT-116^{+/+}-miR-215-5p cells formed significantly smaller tumors compared with HCT-116^{+/+}-control cells 25 days after application into NSG mice ($n = 5$). **b** Volume of *in vivo* formed tumors was significantly smaller in case of HCT-116^{+/+}-miR-215-5p cells compared with HCT-116^{+/+}-control cells. **c** Weight of *in vivo* formed tumors was significantly smaller in case of HCT-116^{+/+}-miR-215-5p cells compared with HCT-116^{+/+}-control cells. **d** Expression levels of miR-215-5p were significantly increased in HCT-116^{+/+}-miR-215-5p tumors compared with HCT-116^{+/+}-control tumors 25 days after initiation of the experiment. **e** Involvement of miR-215-5p in CRC pathogenesis—direct targets of miR-215-5p described first in this study are in red squares, direct targets of miR-215-5p described in previous studies are in brown. * $P < 0.05$, ** $P < 0.01$, CTRL control cells, EMT epithelial-mesenchymal transition, XIAP X-chromosome-linked inhibitor of apoptosis, ZEB2 zinc-finger E-box-binding homeobox 2, DTL denticleless protein homolog, DLG5 discs large homolog 5, TYMS thymidylate synthase, HOXB9 homeobox protein HoxB9, EREG epiregulin

215-5p associated with these processes. From the predicted genes, EREG and HOXB9 have been chosen for further validation. The performed analyses proved these two proteins to be the direct targets of miR-215-5p. Moreover, their expression was significantly upregulated in tumor tissue compared with adjacent healthy tissue. EREG is a member of the epidermal growth factor family that functions as a ligand of EGFR, which is commonly overexpressed in CRC and present one of its main molecular features³⁸. HOXB9 is an important transcription factor contributing to solid tumor invasion and metastasis and its overexpression is associated with poor prognosis^{40, 41}. Interestingly, it was found that EREG promoter contains the HOX-binding site and is a direct transcriptional target of HOXB9⁴². To date, no previous study has confirmed EREG and HOXB9 to be direct targets of miR-215-5p. However, Wu *et al.* identified HOXB9 as a direct target of miR-192, a miRNA from the same family and with a high homology to miR-215-5p⁴³. The most prominent regulatory effect of miR-215-1p on HOXB9 was observed under p53-wild-type conditions, in cell line HCT-116^{+/+}, which could be partly explained by the fact that miR-192^{13, 44} and miR-215⁴⁴ have been shown to be p53-responsive miRNAs. As miR-215-5p has an ability to regulate EGFR ligand EREG and its transcriptional inducer HOXB9, we suggest that the main molecular link between miR-215-5p and CRC cells phenotypes presents the EGFR signaling pathway, which is one of the canonical pathogenic pathways in CRC (Fig. 5e).

In conclusion, we have confirmed a diagnostic and prognostic potential of miR-215-5p in CRC patients in two independent cohorts of patients. In addition, we have proved the tumor-suppressive character of miR-215-5p resulting in reduced proliferation, formation of new colonies, and migration and increased apoptosis. These results correspond with the fact that one miRNA has the ability to regulate several target genes involved in different signaling pathways. Although some of these effects were dependent on the presence of wt-p53, miR-215-5p was also able to slow down the tumor growth independently of this protein. Importantly, two genes—EREG and HOXB9—that are functionally linked to EGFR signaling and are known to be involved in cell proliferation, migration and disease progression have been validated as direct targets of this miRNA. Thus, we believe that miR-215-5p could serve as a potential therapeutic target in CRC.

Materials and methods

Patients and tissue samples

In total, 252 tumor tissue samples from patients with histopathologically verified CRC who had undergone surgery at Masaryk Memorial Cancer Institute (Brno, Czech Republic) from 2004 to 2013, as well as 252 paired

adjacent non-tumor tissues were used for the determination of miR-215-5p expression levels. In addition, 17 samples of corresponding liver metastases obtained from patients with metastatic CRC were used in our study. Further, an independent set of tumor tissues from 196 patients who had undergone the surgery at Santa Lucía General University Hospital (HGUSL, Cartagena, Spain) from 2004 to 2015, as well as 73 paired adjacent non-tumor tissues were involved in the study. All subjects enrolled in the study were of the same ethnicity (European descent) and did not receive any treatment prior to surgery. All patients were followed-up for tumor recurrence at regular intervals and survival time was calculated. Clinical and pathological characteristics were recorded and are summarized in Table 1. Written informed consent was obtained from all participants and the study has been approved by the local Ethical Boards in Masaryk Memorial Cancer Institute and Santa Lucía General University Hospital.

Tissue samples preparation and miRNA isolation

Tissue samples were homogenized (MM301, Retsch GmbH & Co. KG, Germany) and total RNA enriched for small RNAs was isolated using *mirVana* miRNA Isolation Kit (Ambion, Austin, TX, USA) according to the manufacturer's instructions. Concentration and purity of RNA were determined spectrophotometrically by measuring its optical density (A260/280 > 2.0; A260/230 > 1.8) using a Nanodrop ND-1000 (Thermo Fisher Scientific, Waltham, MA, USA).

Reverse transcription and RT-qPCR

For miRNA expression analyses, complementary DNA (cDNA) was synthesized from 10 ng of total RNA using gene-specific primers (has-miR-215-5p; ID 000518, RNU48; ID 001006) according to the TaqMan MicroRNA Assay protocol (Applied Biosystems, Foster City, CA, USA) and real-time PCR was performed using TaqMan Universal PCR Master Mix, NoUmpErase UNG (Applied Biosystems) as described previously¹¹. For quantification of the number of miR-215-5p copies in CRC cells used in our study, a dilution series of synthetic miRNA oligo (IDT, Coralville, IA, USA) were carried out in parallel with qRT-PCR of biological samples to generate an absolute standard curve. MiR-215-5p levels in CRC cells were expressed as number of copies per 100 ng of total RNA purified from CRC cells. For the purposes of gene expression analyses, cDNA was synthesized using 1000 ng of total RNA and the High-Capacity cDNA Reverse Transcription Kit (Applied Biosystems) according to the manufacturer's recommendations. Quantitative PCR was carried out using specific probes for EREG (Hs00914313_m1), HOXB9 (Hs00256886_m1), PMM1 (Hs00160195_m1), CDH1 (Hs01023895_m1), VIM

(Hs00958111_m1), ZEB1 (Hs01566408_m1), ZEB2 (Hs00207691_m1) and GAPDH (glyceraldehyde-3-phosphate dehydrogenase, Hs02758991_g1) (Applied Biosystems). Real-time PCR was performed using the Applied Biosystems 7500 Sequence Detection System.

Cell lines and cell culture

In this study, four human colon carcinoma cell lines were used including HCT-116^{+/+} (CCL-247TM; wt-p53), DLD-1 (CCL-221TM; mut-p53), HT-29 (HTB-38TM; mut-p53), CaCo2 (HTB-37TM; mut-p53) and HCT-116^{-/-} (p53-null derivative). The first four cell lines were obtained from American Type Culture Collection (ATCC), the HCT-116^{-/-} cells were kindly provided by Dr Jiri Kohoutek (Veterinary research institute, Brno, Czech Republic) who gained them from Dr Bert Vogelstein⁴⁵. Cells were cultured in Dulbecco's modified Eagle's medium (DMEM) supplemented with 10% fetal bovine serum, 100 µg ml⁻¹ penicilin, 100 µg ml⁻¹ streptomycin, 0.1 mM non-essential amino acids, 2 mM L-glutamin, 1 mM sodium pyruvate (Invitrogen, Gibco, Carlsbad, CA, USA) in 5% CO₂ at 37 °C. All cell lines were regularly tested with MycoAlert (Lonza Group Ltd, Basel, Switzerland) to ensure the absence of mycoplasma contamination. Authentication of cell lines was done by comparing STR (short tandem repeat) sequences obtained from actual cell lines as determined by Generi Biotech (Hradec Kralove, Czech Republic) with data public available (ATCC, ECACC—European Collection of Authenticated Cell Cultures). Recent STR analysis has been performed within 6 months before the beginning or in the course of the experiments for all cell lines.

Cell transfection

All cell lines were transfected with 10 nM hsa-miR-215-5p mimic (MC10874) or miRNA Mimic, negative control #1 (4464058) or 33 nM hsa-miR-215-5p inhibitor (MH10874) or 33 nM miRNA inhibitor, negative control (4464079) or 30 nM siRNA-negative control (AM4635), siEREG (145900) and siHOXB9 (109525; all from Ambion) 24 h after seeding using Lipofectamine RNAi-MAX transfection reagent (Invitrogen) according to the manufacturer's protocol. Transfection efficiency was evaluated by RT-qPCR.

Cell proliferation and MTT assay

Cells were seeded in triplicates in 10% DMEM without antibiotics in 24-well plates 24 h before transfection and counted 24–96 h after transfection. Cell viability was measured using the MTT assay (Sigma Aldrich, Saint Louis, MO, USA). The absorbance was measured on Multi-Detection Microplate Reader (BIO-TEK, Winooski, VT, USA).

Colony-forming assay

Colony-forming assay was performed using six-well plates pre-coated with 0.75% agarose as the bottom layer, whereas the top layer consisted of 0.35% agarose and tumor cells transfected with miR-215 mimics or control oligonucleotide. After 12–14 days, colonies were stained with crystal violet blue solution (Sigma-Aldrich) and scanned by GelCount (Oxford Optronix, Abingdon, UK). The data were analyzed using ImageJ software (Wayne Rasband, NIH, MD, USA).

Cell cycle analysis and detection of apoptosis

Cell cycle analysis and detection of apoptosis were performed using flow cytometry as described previously¹¹. The cells were analyzed 72 and 96 h post-transfection.

Scratch wound migration assay

The migration of cells was analyzed using scratch wound migration assay. Cells were seeded on six-well plates and the cell monolayer was wounded 24 h after the transfection. The migration was measured at time 0 and 24 h post-wounding using a microscope Nikon Diaphod 300 INV (10 ×) and camera Canon Power shot A95. Images were analyzed by the Tscratch software (CSElab, ETH Zurich, Switzerland).

Transwell migration assay

Transwell migration assay was performed using 8 µm transwell inserts for 24-well plates (Costar, Corning Incorporated, Corning, NY, USA) and staining with Hoechst 33342 (Invitrogen). The migrated cells were counted using fluorescence microscope and ImageJ software (Wayne Rasband).

Luciferase assay

For luciferase reporter assay, MISSION 3'-UTR Lenti GoClone HOXB9 (HUTR10238) and appropriate negative control (HUTR001C) from SwitchGear Genomics (Carlsbad, CA, USA) were used and the viral particles were added at MOI (multiplicity of infection) = 2.5. In case of EREG, 1 µg of pEZX-MT05 vector containing UTR for EREG (HmiT004978) or appropriate control vector (CmiT000001-MT05) were transfected into DLD-1 cells using EndoFectin Plus Transfection Reagent (GeneCopoeia, Rockville, MD, USA). The luciferase activity was measured using the MISSION LightSwitch Luciferase Assay Reagent (Sigma Aldrich) or SecretePair Dual Luminescence assay kit (GeneCopoeia), respectively, using FLUOstar Omega Microplate reader (BMG Labtech, Ortenberg, Germany).

Western blotting

Cells were seeded in 60 mm plates and 48 h after transfection they were lysed with RIPA buffer (Sigma-

Aldrich) containing Complete mini protease and phosphatase inhibitor cocktail tablets (Roche, Basel, Switzerland). Protein quantification was performed using the Bradford protein assay (Bio-Rad, Hercules, CA, USA) and 10 μg of lysate was loaded per lane. Proteins were resolved by 8 or 10% sodium dodecyl sulfate–polyacrylamide gel electrophoresis gel and wet transferred to polyvinylidene difluoride membrane (EMD Millipore, Billerica, MA, USA). The signals were visualized by ECL Prime Western blotting Detection Reagent (Amersham, Piscataway, NJ, USA) and exposed to AGFA Curix X-ray film (AGFA, Mortsel, Belgium). The following Ab were used: anti-HOXB9 (1:100, mouse, sc-398500) from Santa Cruz Biotechnology Inc. (Dallas, TX, USA) and anti-EREG (1:1000, rabbit, 12048 S), anti-PARP (1:1000, rabbit, 9542 S) and anti- β -tubulin (1:2000, rabbit, 2146 S) from Cell Signaling Technology (Danvers, MA, USA).

Generation of stable cell line overexpressing miR-215-5p

Stable transfectants were generated using OriGene's pCMV6-Mir vectors with miR-215-5p precursor or control sequence and TurboFectin 8.0 (OriGene Technologies, Rockville, MD, USA). Stable clones were selected using 300 $\mu\text{g ml}^{-1}$ G418 (Sigma Aldrich). The stable expression of miR-215-5p was evaluated by RT-qPCR.

In vivo tumorigenicity assay

Five NSG mice (males, 8–10 weeks old, 21–26 g, initially obtained from The Jackson Laboratory, Bar Harbor, USA) were housed and monitored in individually ventilated cage system (Techniplast, Buguggiate, Italy) with ad libitum access to water and feeding. The assay was performed according to the protocol described previously^{46, 47}. Tumors have been palpable since day 14 and mice were sacrificed on day 25. During the experiment, tumor growth and animal behavior were individually monitored. Animal experiments were performed in accordance with national and EU animal welfare legislation and all procedures were approved by institutional (Masaryk University, Brno) and national ethics committees.

Data normalization and statistical analyses

The threshold cycle data were calculated by QuantStudio 12 K Flex software using the default threshold settings. All real-time PCR reactions were run in triplicates and average threshold cycle and SD values were calculated. The average expression levels of miR-215-5p in tumor and adjacent non-tumor tissues, as well as in the cell lines were normalized using RNU48 as a reference gene, the expression of EREG and HOXB9 was normalized using PMM1 (in case of tissue samples) or GAPDH (in case of cell lines) as a reference genes; subsequently, all data were transformed by the $2^{-\Delta\text{Ct}}$ method. Statistical differences between the levels of miR-215-5p in tumor

and non-tumor tissues were evaluated by the non-parametric Wilcoxon test for paired samples. Furthermore, Mann–Whitney *U*-test was used to analyze the correlation between miR-215-5p expression levels and clinical–pathological features of the patients. Survival analyses were performed using the log-rank test and Kaplan–Meier plots approach. For *in vitro* and *in vivo* analyses, the two-sided Student's *t*-test was used to compare the mean values between two groups. Data are presented as the mean values with SD unless otherwise noted (all *in vitro* measurements were repeated three times). All calculations were performed using GraphPad Prism version 5.00 (GraphPad Software, San Diego, CA, USA). *P*-values of <0.05 were considered statistically significant.

Acknowledgements

This work was supported by grant project GACR 16-18257S, the project CEITEC 2020 (LQ1601) provided by the Ministry of Education Youth and Sports of the Czech Republic and projects MUNI/A/1284/2015 and MUNI/11/InGA09/2014. The authors thank Helena Polakova, Andrej Besse and Jan Verner for their excellent technical assistance.

Author details

¹Central European Institute of Technology, Masaryk University, Brno, Czech Republic. ²Department of Comprehensive Cancer Care, Masaryk Memorial Cancer Institute, Faculty of Medicine, Masaryk University, Brno, Czech Republic. ³Department of Pharmacology, Faculty of Medicine, Masaryk University, Brno, Czech Republic. ⁴Department of Clinical Analysis, Santa Lucia University Hospital, Cartagena, Spain. ⁵Department of Pathology, Santa Lucia University Hospital, Cartagena, Spain

Competing interests

The authors declare no competing financial interests.

Publisher's note: Springer Nature remains neutral with regard to jurisdictional claims in published maps and institutional affiliations.

Supplementary information

The online version of this article (doi:10.1038/s41389-017-0006-6) contains supplementary material.

Received: 8 May 2017 Revised: 16 September 2017 Accepted: 18 September 2017

Published online: 04 December 2017

References

1. Ferlay, J. et al. Cancer incidence and mortality worldwide: sources, methods and major patterns in GLOBOCAN 2012. *Int. J. Cancer* **136**, E359–E386 (2015).
2. Sana, J., Faltejskova, P., Svoboda, M. & Slaby, O. Novel classes of non-coding RNAs and cancer. *J. Transl. Med.* **10**, 103 (2012).
3. Gomes, A. Q., Nolasco, S. & Soares, H. Non-coding RNAs: multi-tasking molecules in the cell. *Int. J. Mol. Sci.* **14**, 16010–16039 (2013).
4. Crea, F., Clermont, P. L., Parolia, A., Wang, Y. & Helgason, C. D. The non-coding transcriptome as a dynamic regulator of cancer metastasis. *Cancer Metastasis Rev.* **33**, 1–16 (2014).
5. Joh, R. I., Palmieri, C. M., Hill, I. T. & Motamedi, M. Regulation of histone methylation by noncoding RNAs. *Biochim. Biophys. Acta* **1839**, 1385–1394 (2014).
6. Lai, E. C. Micro RNAs are complementary to 3' UTR sequence motifs that mediate negative post-transcriptional regulation. *Nat. Genet.* **30**, 363–364 (2002).

7. Cho, W. C. S. OncomiRs: the discovery and progress of microRNAs in cancers. *Mol. Cancer* **6**, 60 (2007).
8. Calin, G. A. & Croce, C. M. MicroRNA signatures in human cancers. *Nat. Rev. Cancer* **6**, 857–866 (2006).
9. Slaby, O., Svoboda, M., Michalek, J. & Vyzula, R. MicroRNAs in colorectal cancer: translation of molecular biology into clinical application. *Mol. Cancer* **8**, 102 (2009).
10. Amankwata, E. B. et al. MicroRNA-224 is associated with colorectal cancer progression and response to 5-fluorouracil-based chemotherapy by KRAS-dependent and -independent mechanisms. *Br. J. Cancer* **112**, 1480–1490 (2015).
11. Faltejskova, P. et al. Identification and functional screening of microRNAs highly deregulated in colorectal cancer. *J. Cell Mol. Med.* **16**, 2655–2666 (2012).
12. Necela, B. M., Carr, J. M., Asmann, Y. W. & Thompson, E. A. Differential expression of microRNAs in tumors from chronically inflamed or genetic (APC (Min/+)) models of colon cancer. *PLoS ONE* **6**, e18501 (2011).
13. Braun, C. J. et al. p53-Responsive microRNAs 192 and 215 are capable of inducing cell cycle arrest. *Cancer Res.* **68**, 10094–10104 (2008).
14. Song, B. et al. Molecular mechanism of chemoresistance by miR-215 in osteosarcoma and colon cancer cells. *Mol. Cancer* **9**, 96 (2010).
15. Boni, V. et al. miR-192/miR-215 influence 5-fluorouracil resistance through cell cycle-mediated mechanisms complementary to its post-transcriptional thymidilate synthase regulation. *Mol. Cancer Ther.* **9**, 2265–2275 (2010).
16. Li, S. et al. MicroRNA-215 inhibits relapse of colorectal cancer patients following radical surgery. *Med. Oncol. Northwood Lond. Engl.* **30**, 549 (2013).
17. Agarwal, V., Bell G. W., Nam J.-W. & Bartel, D.P. Predicting effective microRNA target sites in mammalian mRNAs. *eLife* **4**, e05005 (2015).
18. Maragkakis, M. et al. DIANA-microT Web server upgrade supports Fly and Worm miRNA target prediction and bibliographic miRNA to disease association. *Nucleic Acids Res.* **39**, W145–W148 (2011).
19. Rehmsmeier, M., Steffen, P., Höchsmann, M. & Giegerich, R. Fast and effective prediction of microRNA/target duplexes. *RNA* **10**, 1507–1517 (2004).
20. Miranda, K. C. et al. A pattern-based method for the identification of MicroRNA binding sites and their corresponding heteroduplexes. *Cell* **126**, 1203–1217 (2006).
21. John, B. et al. Human microRNA targets. *PLoS Biol.* **2**, e363 (2004).
22. Riese, D. J. & Cullum, R. L. Epiregulin: roles in normal physiology and cancer. *Semin. Cell Dev. Biol.* **28**, 49–56 (2014).
23. Zhan, J. et al. Elevated HOXB9 expression promotes differentiation and predicts a favourable outcome in colon adenocarcinoma patients. *Br. J. Cancer* **11**, 883–893 (2014).
24. Bonfrate, L. et al. MicroRNA in colorectal cancer: new perspectives for diagnosis, prognosis and treatment. *J. Gastrointest. Liver Dis.* **22**, 311–320 (2013).
25. Hollis, M. et al. MicroRNAs potential utility in colon cancer: early detection, prognosis, and chemosensitivity. *World J. Gastroenterol.* **21**, 8284–8292 (2015).
26. Stiegelbauer, V. et al. MicroRNAs as novel predictive biomarkers and therapeutic targets in colorectal cancer. *World J. Gastroenterol.* **20**, 11727–11735 (2014).
27. Karaayvaz, M. et al. Prognostic significance of miR-215 in colon cancer. *Clin. Colorectal. Cancer* **10**, 340–347 (2011).
28. Slattery, M. L. et al. An evaluation and replication of miRNAs with disease stage and colorectal cancer-specific mortality. *Int. J. Cancer* **137**, 428–438 (2015).
29. Zhang, J. X. et al. Prognostic and predictive value of a microRNA signature in stage II colon cancer: a microRNA expression analysis. *Lancet Oncol.* **14**, 1295–1306 (2013).
30. Yang, J. et al. Expression analysis of microRNA as prognostic biomarkers in colorectal cancer. *Oncotarget* **8**, 52403–52412 (2017).
31. Georges, S. A. et al. Coordinated regulation of cell cycle transcripts by p53-inducible microRNAs, miR-192 and miR-215. *Cancer Res.* **68**, 10105–10112 (2008).
32. Banks, D. et al. L2DTL/CDT2 and PCNA interact with p53 and regulate p53 polyubiquitination and protein stability through MDM2 and CUL4A/DDB1 complexes. *Cell Cycle (Georgetown, TX)* **5**, 1719–1729 (2006).
33. Jeanes, A., Gottardi, C. J. & Yap, A. S. Cadherins and cancer: how does cadherin dysfunction promote tumor progression? *Oncogene* **27**, 6920–6929 (2008).
34. Nechiporuk, T., Fernandez, T. E. & Vasioukhin, V. Failure of epithelial tube maintenance causes hydrocephalus and renal cysts in Dlg5^{-/-} mice. *Dev. Cell* **13**, 338–350 (2007).
35. Ge, G. et al. miR-215 functions as a tumor suppressor in epithelial ovarian cancer through regulation of the X-chromosome-linked inhibitor of apoptosis. *Oncol. Rep.* **35**, 1816–1822 (2016).
36. Ye, M. et al. Curcumin promotes apoptosis by activating the p53-miR-192-5p/215-XIAP pathway in non-small cell lung cancer. *Cancer Lett.* **357**, 196–205 (2015).
37. White, N. M. A. et al. mRNA profiling in metastatic renal cell carcinoma reveals a tumour-suppressor effect for miR-215. *Br. J. Cancer* **105**, 1741–1749 (2011).
38. Hou, Y. et al. miR-215 functions as a tumor suppressor and directly targets ZEB2 in human non-small cell lung cancer. *Oncol. Lett.* **10**, 1985–1992 (2015).
39. Li, Q. W. et al. MicroRNA-215 functions as a tumor suppressor and directly targets ZEB2 in human pancreatic cancer. *Genet. Mol. Res.* **14**, 16133–16145 (2015).
40. Huang, K. et al. Overexpression of HOXB9 promotes metastasis and indicates poor prognosis in colon cancer. *Chin. J. Cancer Res.* **26**, 72–80 (2014).
41. Shrestha, B. et al. Homeodomain containing protein HOXB9 regulates expression of growth and angiogenic factors, facilitates tumor growth in vitro and is overexpressed in breast cancer tissue. *FEBS J.* **279**, 3715–3726 (2012).
42. Hayashida, T. et al. HOXB9, a gene overexpressed in breast cancer, promotes tumorigenicity and lung metastasis. *Proc. Natl. Acad. Sci. USA* **107**, 1100–1105 (2010).
43. Wu, S. Y. et al. A miR-192-EGR1-HOXB9 regulatory network controls the angiogenic switch in cancer. *Nat. Commun.* **7**, 11169 (2016).
44. Song, B. et al. miR-192 Regulates dihydrofolate reductase and cellular proliferation through the p53 microRNA circuit. *Clin. Cancer Res.* **14**, 8080–8086 (2008).
45. Bunz, F. et al. Requirement for p53 and p21 to sustain G2 arrest after DNA damage. *Science* **282**, 1497–1501 (1998).
46. Morton, C. L. & Houghton, P. J. Establishment of human tumor xenografts in immunodeficient mice. *Nat. Protoc.* **2**, 247–250 (2007).
47. McKay, J. A. et al. Evaluation of the epidermal growth factor receptor (EGFR) in colorectal tumours and lymph node metastases. *Eur. J. Cancer* **38**, 2258–2264 (2002).